E6-2007-186

O. Zeynalova[1], Sh. Zeynalov[1,2], F. -J. Hambsch[2], S. Oberstedt[2]

DIGITAL SIGNAL PROCESSING ALGORITHMS FOR NUCLEAR PARTICLE SPECTROSCOPY

Submitted to «NIM»

[1]Joint Institute for Nuclear Research, Joliot Curie 6, Dubna, Moscow region, Russia
[2] EC-JRC-Institute for Reference Materials and Measurements, Retieseweg 111, B-2440 Geel, Belgium

Зейналова О. и др. E6-2007-186
Алгоритмы для цифровой обработки сигналов
при спектрометрии ядерных частиц

Рассмотрены алгоритмы цифровой обработки сигналов и метод исключения наложений импульсов при спектрометрии ядерных частиц для импульсов, дискретизованных с фиксированной частотой. Процедуры обработки сигналов сформулированы в виде рекурсивных процедур, удобных для программирования с использованием современных алгоритмических языков. Исследовалось влияние числа бит амлитудно-цифрового преобразователя на величину отношения сигнал/шум спектрометра. Разработаны и испытаны алгоритмы цифрового спектрометрического усилителя с трапецеидальным и CR-RCn формированием, устройства исключения наложений и процедура коррекции «баллистического дефицита». Испытания спектрометрических характеристик проведены с использованием детектора гамма-квантов из сверхчистого германия. Изначально указанные алгоритмы разрабатывались для спектроскопии осколков деления ядер, но наиболее полное исследование их характеристик оказалось возможным с применением детектора высокого разрешения. Исследовалось влияние метода исключения наложений на разрешение спектрометра в зависимости от расстояния между исследуемыми импульсами.

Работа выполнена в Лаборатории информационных технологий ОИЯИ.

Препринт Объединенного института ядерных исследований. Дубна, 2007

Zeynalova O. et al. E6-2007-186
Digital Signal Processing Algorithms for Nuclear Particle Spectroscopy

Digital signal processing algorithms for nuclear particle spectroscopy are described along with a digital pile-up elimination method applicable to equidistantly sampled detector signals pre-processed by a charge-sensitive preamplifier. The signal processing algorithms are provided as recursive one- or multi-step procedures which can be easily programmed using modern computer programming languages. The influence of the number of bits of the sampling analogue-to-digital converter on the final signal-to-noise ratio of the spectrometer is considered. Algorithms for a digital shaping-filter amplifier, for a digital pile-up elimination scheme and for ballistic deficit correction were investigated using a high purity germanium detector. The pile-up elimination method was originally developed for fission fragment spectroscopy using a Frisch-grid back-to-back double ionization chamber and was mainly intended for pile-up elimination in case of high alpha-radioactivity of the fissile target. The developed pile-up elimination method affects only the electronic noise generated by the preamplifier. Therefore, the influence of the pile-up elimination scheme on the final resolution of the spectrometer is investigated in terms of the distance between piled-up pulses. The efficiency of the developed algorithms is compared with other signal processing schemes published in literature.

The investigation has been performed at the Laboratory of Information Technologies, JINR.

Preprint of the Joint Institute for Nuclear Research. Dubna, 2007

INTRODUCTION

The basic element of a nuclear spectrometer is a detector combined with a charge-sensitive preamplifier. The measurement of the kinetic energy of a radiation particle relies on the processing of the electric current pulse created by the motion of the free electrons/holes released during the ionization of the detector material. The time dependence of the detector current also conveys information on the ionization density along the ionizing particles' deceleration path. The total number of free electrons/holes is proportional to the particle kinetic energy, which can be evaluated as the integral of the current flown through the detector. The step-like pulse at the output of a charge-sensitive preamplifier (CSPA) is the result of an integration of the detector current. The height of the pulse is proportional to the total charge produced during the deceleration of the charged particle. This pulse height can be measured as the difference between the baseline (before the particle hits the detector) and the peaking value (after total charge collection was done) of the pulse after filtering out the useless high frequency components with the help of a shaping-filter amplifier (SFA). This principle is implemented in commercially available nuclear electronic modules performing signal processing which can be represented as a sequence of mathematical procedures applied to the waveform of a continuous signal. Sometimes, when pulse shape information is needed, the analysis of the detector current signal can be more convenient. The current pulse can be converted into a step pulse by digital integration and vice versa. The output pulse of the SFA can have either a Gaussian or flat top pulse shape that can be used as the input to a peak-sensing analogue-to-digital converter (ADC) for a pulse height analysis. From a mathematical point of view, one can consider the signal evolution from the detector to the ADC as a sequence of transformations that can be described by precisely defined mathematical expressions. For example, the CSPA integrates the input current pulse; the SFA convolutes the output signal of the preamplifier with a kernel function defined by the shaping parameters of the SFA; and the ADC converts the peak value of the shaped pulse to a digital output value. Recently, using waveform digitizer (WFD), the above mentioned mathematical transformations implemented in analogue electronic modules can be implemented software-wise using digital signal processing (DSP) algorithms. Some examples of the implementation of

DSP techniques to nuclear particle spectroscopy are reported in Refs. 1–5, where the analogue pulse processing modules with continuous time signals were replaced by direct calculations with sampled signals — discrete values taken from a continuous signal at equidistantly separated points. According to Shannon's theorem, if the signal sampling was done properly, both the sampled and continuous forms of the signal representation are equivalent to each other. In practice the difference between the two representations depends on the precision of the analogue-to-digital conversion.

HARDWARE AND SOFTWARE USED IN MEASUREMENTS

Detector pulses were digitized using a TDS3054B digital storage oscilloscope from Tektronix Inc. as shown in Fig. 1. The TDS3054B allowed signal digitization with an accuracy of 8 bit and with a frequency of up to $5 \cdot 10^9$ samples/sec. Four waveforms of 10000 samples each can be simultaneously recorded in the local memory of the oscilloscope, controlled by a remote PC via Ethernet connection. Data exchange between the oscilloscope and the PC was facilitated by the TekVISA [6] software library easily accessible from the Tektronix Inc. company web site. Both the data acquisition and the data analysis software were developed using Microsoft Visual C++ for Windows XP. Let us consider, for example, a high-purity germanium (HPGe) detector irradiated by a ^{60}Co calibration source. Detector pulses after being processed by a CSPA (with -3dB bandwidth of ~ 15 MHz) were digitized by the oscilloscope with 250 MHz and 8 bit (256 levels) accuracy. According to Shannon's theorem the digitization is a lossless procedure if the signal sampling frequency is more than 2*F, where F is the signal bandwidth. Let us consider Fig. 1 where the block diagram of the CSPA is presented to demonstrate the transformation of the detector signal. Let t being the time interval passed from the start of the measurement when the particle hits the detector and $I(t)$ is the instant value of the electric current flowing through the detector at time t. Assuming a particle entering the detector at $t = 0$, the following relation between the detector current and the preamplifier output voltage $V(t)$ is valid:

$$V(t) = \int_0^\infty I(\tau)h(t-\tau)d\tau. \tag{1}$$

The measured output $V(t)$ can be used directly for the determination of the total charge created by the particle assuming that the current pulse duration is short enough and $h(\tau) \sim$ const. In real systems the finite pulse duration leads to a systematic error, the so-called ballistic deficit, depending on the shape of

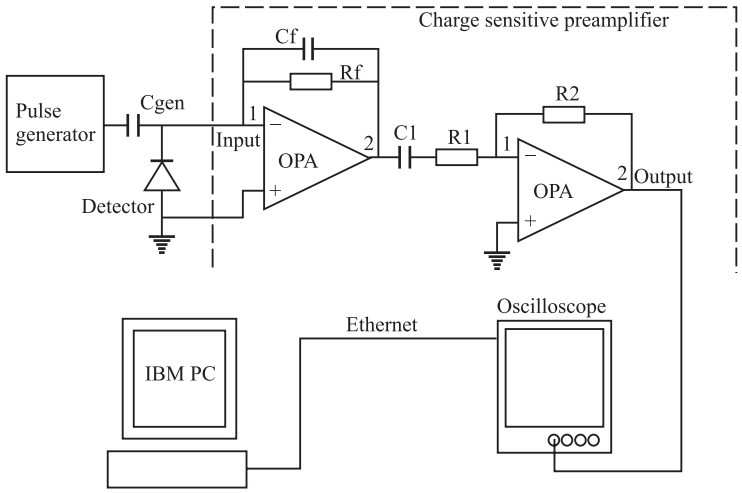

Fig. 1. Generalized block diagram of a charge-sensitive preamplifier along with the data acquisition system

$I(\tau)$. Thanks to digitization the solution of Eq. (1) with respect to $I(\tau)$ becomes possible allowing a direct evaluation of the detector current and the total charge. Inversion of Eq. (1) yields:

$$I(t) = \int_0^\infty V(\tau)H(t-\tau)d\tau. \tag{2}$$

As follows from Eq. (2), the electric current flowing through the detector can be found if $H(t)$ is a known function and $V(t)$ has been measured. The function $H(t)$ usually can be determined using a precision pulse generator in a separate measurement, and it is supposed to be a stable characteristic of a given preamplifier.

MAIN PROPERTIES OF SAMPLED AND CONTINUOUS SIGNAL REPRESENTATIONS

We suppose that all functions in Eq. (2) and further on in this work are continuous functions of the argument and they belong to the functional space L_2 (continuous functions, having continuous derivatives of first and second orders). However, the sampling procedure converts continuous functions into sequences of discrete numbers taken at equidistantly spaced points in time. Let us now consider the sampling procedure of the $V(t)$ function in some detail, presuming that the sampling frequency is chosen to comply with the requirements of Shannon's

theorem. In addition we assume a measurement is made with an ideal WFD taking an instant value of the signal with infinite resolution. Such kind of digitization cannot be realized in practice, but as it was shown in Ref. 7, the effects related to a noninstant conversion can be taken into account by the convolution of the instantly sampled signal with a kernel function well defined by the width of the time window needed for the analogue-to-digital conversion at the sampling point. A mathematical model of the ideal sampling can be represented with the following equation:

$$V_S(t) = V(t)p(t) = V(t) \sum_{m=-\infty}^{\infty} \delta(t - \frac{m}{F_S}), m = ..., -2, -1, 0, 1, 2, ..., \quad (3)$$

where, $\delta(t)$ is Dirac's delta function. Application of the Fourier transform to Eq. (3) gives:

$$\hat{V}_S(f) = \hat{V}(f) * \hat{P}(f) = \sum_{k=-\infty}^{\infty} \hat{V}(f + kF_S), \quad (4)$$

where the symbol * was used for the convolution operation and $\hat{V}_S(f)$ is the Fourier transform of the function$V_S(t)$. Equation (4) represents the Fourier transform of the $V_S(t)$ signal, which is a periodical repetition of $\hat{V}_S(f)$ with a period of 1/F_S. If the sampling frequency is high enough to prevent spectrum overlap between adjacent periods, then each interval contains the exact copy of $\hat{V}_S(f)$. By multiplying Eq. (4) with the rectangular function $\Pi(f)$ equal to 1 inside the interval [0, F_S] and zero otherwise, one can obtain a function with the same Fourier transform as for $V(t)$. Finally, the following equation known as Shannon's equation, provides the rule for reconstructing the continuous signal from its samples:

$$V_S(t) = \sum_{m=-\infty}^{\infty} V(\frac{m}{F_S}) sinc(F_S(t - \frac{m}{F_S})), \quad sinc(x) = \frac{\sin(\pi x)}{\pi x}. \quad (5)$$

It should be noted that $sinc(x)$ is the Fourier transform of the rectangular function $\Pi(f)$ which is usually called the window function. The $sinc(x)$ function in turn is usually called the time resolution function. For practical applications, a Gaussian type window function, for example, is sometimes more preferable because of its nonoscillating behaviour. It should be noted that in practical applications always sampled functions are used in calculations. The continuous presentation of a sampled signal using Eq. (5) provides the means to increase the sampling frequency when it can be necessary for calculations with the waveforms.

The finite resolution of the WFD can be treated as an additional source of noise, called quantization noise. For example, the absolute accuracy of samples

$V(\frac{m}{F_S})$ taken by an eight-bit WFD in Eq. (5) is $1/N$, where $N = 2^M$ is the number of quantization levels. Hence, each sample has a statistical error homogenoeusly distributed in the [0, $1/256$] interval. If the investigated signal is a sine wave with amplitude slightly below the clipping range of the WFD, then the theoretical root mean square (RMS) signal to quantization noise ratio (SNR) measured within the Nyquist bandwidth according to Ref. 8 is given by:

$$\mathrm{SNR}_{dB} = 20\log_{10}(\frac{\mathrm{RMS}_{\mathrm{Signal}}}{\mathrm{RMS}_{\mathrm{Noise}}}) = 6.02M + 1.76dB, \tag{6}$$

where dB stands for decibel, and, when used with signals, is a dimensionless quantity that indicates the ratio of the signal RMS to the RMS of the noise. In practice, the fluctuation of the quantization level widths of a real WFD produces additional noise which can be taken into account as a reduction of the physical number of bits in accordance with the solution of the following equation taken from Ref. 8:

$$\mathrm{ENOB} = \frac{\mathrm{SNR}_{\mathrm{Actual}} - 1.76dB}{6.02}. \tag{7}$$

The effective number of bits (ENOB) can be measured by stimulating the input of the WFD by a sine wave with the frequency compliant to the Nyquist criterion. Such a sine wave was applied to the preamplifier input as shown in Fig. 1. After a number of samples were collected, a least-squares fitting procedure was used to evaluate the actual SNR. Then ENOB was found using Eq. (7) and the WFD was considered as an ideal device with an ENOB not necessarily being an integer number. It should be noted, if Eq. (7) is used for a unipolar signal, then the ENOB value turns out to be one bit greater than calculated with a bipolar sine wave.

DESCRIPTION OF THE DIFFERENTIATION AND SHAPING ALGORITHMS

Equation (1), providing the relation between the preamplifier output signal and the detector current stimulated by the ionizing particle, can be used as a starting point for the determination of the particle's kinetic energy. In practice, the function $h(t-\tau)$can be represented analytically as:

$$h(t-\tau) = \frac{1}{\alpha}\exp\left(-(t-\tau)/\alpha\right) \text{ for } t \geqslant \tau, \text{ and } h(t-\tau) = 0, \text{ for } t < \tau. \tag{8}$$

The parameter α is the decay time of the preamplifier and is in the range of 50–100 μs. A δ-function-like current pulse applied to a charge sensitive preamplifier input produces according to Eq. (1) a step-like output signal with fast rise time and exponential decay time α (see left part of Fig. 2). The height of the pulse is

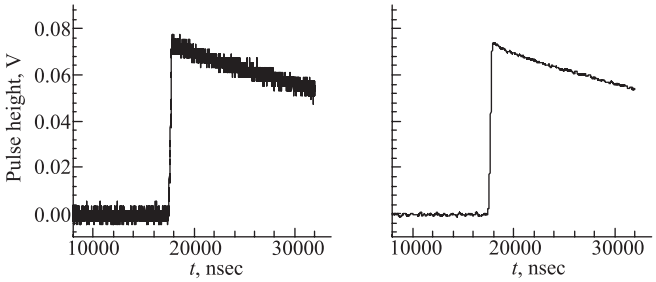

Fig. 2. Original signal $V(t)$ (left part) and smoothed signal $v(t)$ (right part) using Eq. (9)

proportional to the total charge composing the current pulse, hence to the kinetic energy of the ionizing particle. In the present measurement, the output signal of the preamplifier was digitized and stored for further off-line DSP analysis. As mentioned above, according to Shannon's theorem, sampled and continuous representations of the signal are equivalent to each other if the signal sampling was made correctly [5, 7]. Considering the transformation of Eq. (1) as follows:

$$v(t) = \frac{1}{\sqrt{\pi\sigma^2}} \int_0^\infty V(\tau) \exp\,(-\frac{(t-\tau)^2}{2\sigma^2}) d\tau = \int_0^\infty i(\vartheta) h(t-\vartheta) d\vartheta, i(\vartheta) =$$

$$= \frac{1}{\sqrt{\pi\sigma^2}} \int_0^\infty I(\xi) \exp\,(-\frac{(\vartheta-\xi)^2}{2\sigma^2}) d\xi, \quad (9)$$

one finds that Eq. (9) is the smoothed version of Eq. (1) with the following smoothing filter kernel function $S(\tau) = \frac{1}{\sqrt{\pi\sigma^2}} \exp\,(-\frac{\tau^2}{2\sigma^2})$. A smoothing on the right-hand side of Eq. (1) is necessary for noisy signals to prevent large fluctuations in the solution, but it is not strictly required. The effect of filtering is demonstrated in Fig. 2, where both signals representing $v(t)$ and $V(t)$ are given for comparison. A smoothed function $i(t)$ for the detector current can be found from Eq. (9) using the following recursive expression representing a differentiation

$$i_k = \lambda\nu_k - \nu_{k-1}, k = 0, 1, 2, ...N, \quad (10)$$

where $i_k = i(t_k)$, $\nu_k = \nu(t_k)$ are values taken at the sampling points t_k, $i_0 = 0$, and $\lambda = \exp\,(1/\alpha)$ is defined by the used preamplifier. The time dependence of the detector current found with the help of Eq. (10) is shown in Fig. 3. Integrating this current signal over time according to expression

$$Q(t) = \int_0^t i(\vartheta) d\vartheta, \quad (11)$$

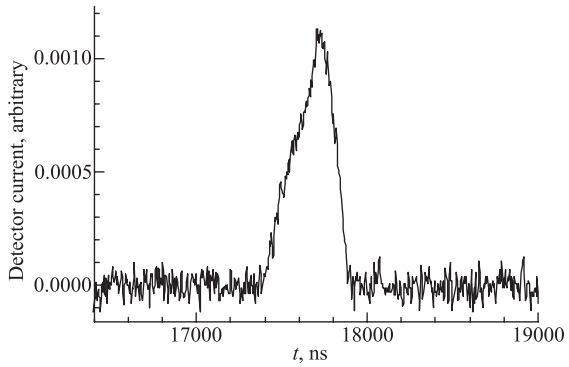

Fig. 3. Current pulse $i(t)$ found as the solution of Eq. (9) using the recursive Eq. (10)

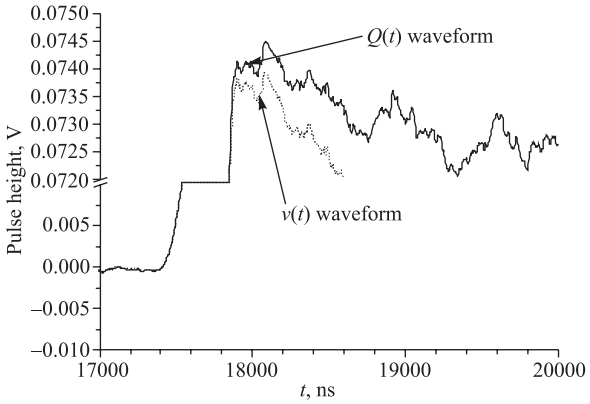

Fig. 4. Signal $v(t)$ and the solution of Eq. (11) $Q(t)$. The ballistic deficit value can be seen as the difference at the peaking points of the two signals

leads to the total charge flown through the detector as the peak value of the step pulse $Q(t)$. Both $Q(t)$ and ν(t) are presented in Fig. 4 for demonstrating the «ballistic deficit» that can be seen as the difference between the two signal peaks (this is difficult to see). In the optimal analogue signal processing procedure [8, 9], the signal $Q(t)$ first passed the C-R (circuit consisting of a serially linked capacitance — C and a resistance — R as shown in the left-hand side of Fig. 5) differentiator with the transfer function as follows:

$$Df(\tau) = \delta(\tau) - \frac{1}{A}\exp\left(-\frac{\tau}{A}\right), \tag{12}$$

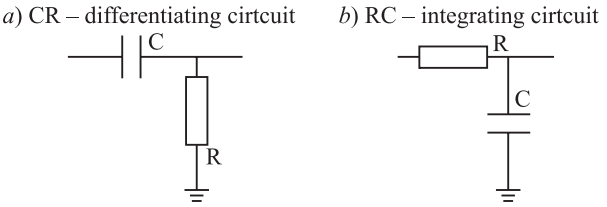

Fig. 5. Differentiating (a) and integrating circuits (b) made of a resistor and a capacitor

where $\delta(\tau)$ is Dirac's delta-function and A is a shaping constant. Usually differentiation is followed by 3–4 successive R-C (circuit consisting of a serially linked resistance — R and a capacitance — C as shown in the right side of Fig. 5) integrations with the following transfer function

$$\mathrm{Int}(\tau) = \frac{1}{A}\exp\left(-\frac{\tau}{A}\right). \tag{13}$$

After differentiation, the step-like function is transformed into an exponential decay function with the peak value proportional to the total charge value collected on the detector electrode. Successive integrations are needed to improve the signal-to-noise ratio resulting in an almost Gaussian shaped pulse. Historically, signal processing using Eqs. (12) and (13) was derived by optimization of the SNR using signal filtering after differentiation [8]. The following equation provides the mathematical description of the transformations (12) and (13):

$$V^{\mathrm{Out}}(t) = \int_0^t \frac{dV^{\mathrm{In}}(\tau)}{d\tau} W(t-\tau)d\tau = \\ = V^{\mathrm{In}}(t)W(0) - \int_0^t V^{\mathrm{In}}(\tau)\frac{dW(t-\tau)}{d\tau}d\tau. \tag{14}$$

For example, it can be easily verified that the convolution of $\dfrac{dV^{\mathrm{In}}(t)}{dt}$ with the weighting function

$$W(\tau) = \frac{1}{A}\exp\left(-\frac{\tau}{A}\right) \tag{15}$$

is equivalent to the transformations given by Eqs. (12) and (13). The peak value of $V^{\mathrm{Out}}(t)$, corresponding to the total measured charge of the ionizing particle, is proportional to the particle's kinetic energy. Changing the weighting function$W(t)$ one can obtain different signal shape and signal processing schemes optimized for a particular experiment, and may be chosen as a compromise between counting rate and resolution. One can verify the validity of the following

transformation:

$$V^{\mathrm{In}}(t)W(0) - \int_0^\infty V^{\mathrm{In}}(\tau)\frac{dW(t-\tau)}{d\tau}d\tau = V^{\mathrm{In}}(t) - \int_0^\infty V^{\mathrm{In}}(\tau)\frac{dW(t-\tau)}{d\tau}d\tau. \tag{16}$$

Using the substitution

$$V_k^{\mathrm{In}} = V^{\mathrm{In}}(k\Delta), V_k^{\mathrm{Out}} = V^{\mathrm{Out}}(k\Delta) \text{ and } V_k^{\mathrm{Int}} = \int_0^\infty V^{\mathrm{In}}(\tau)\frac{dW(k\Delta-\tau)}{d\tau}d\tau$$

one can get the following relations from Eq. (16):

$$V_{k+1}^{\mathrm{Int}} = V_k^{\mathrm{Int}} \times A + V_k^{\mathrm{In}}, V_k^{\mathrm{Out}} = V_k^{\mathrm{Int}} - V_k^{\mathrm{In}}. \tag{17}$$

Applying N subsequent integrations using relation $V_{k+1}^{\mathrm{Int}} = V_k^{\mathrm{Int}} \times A + V_k^{\mathrm{In}}$, where at each next step the output signal from the previous step is treated as the input signal for the next step, is identical to passing of the signal through a CR-RC^n filter. Figure 6 illustrates how a step like pulse is transformed when passed through the CR-RC^4 filter. For a trapezoidal filter as shown in Fig. 7 the following recursive expression was obtained:

$$V_{k+1}^{\mathrm{Out}} = V_k^{\mathrm{Out}} - (V_{k-T+1}^{\mathrm{In}} + V_{k-T-A}^{\mathrm{In}} - V_{k-1}^{\mathrm{In}} + V_{k-2T+1-A}^{\mathrm{In}}), \tag{18}$$

where the meaning of constants A, T is indicated in Fig. 7. The output pulses of the CR-RC^4 (A = 4000 ns) and trapezoid filters (T = 4000 ns, A = 800 ns) are

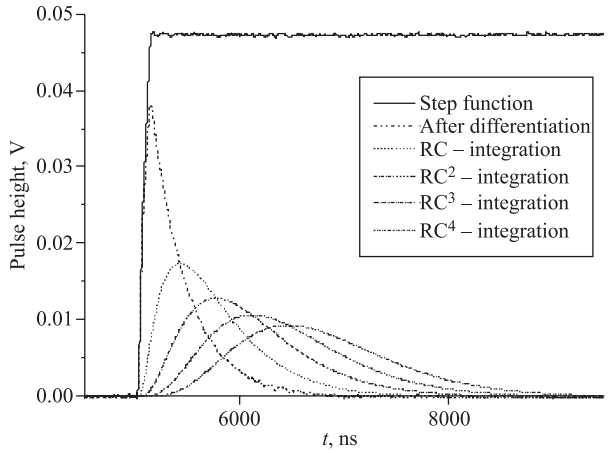

Fig. 6. Passage of a step-like pulse through the CR-RC^4 filter

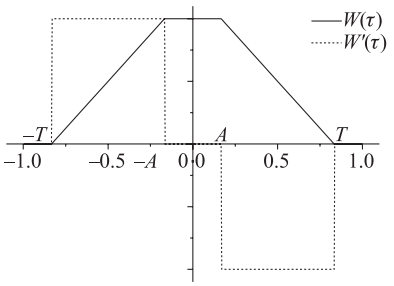

Fig. 7. Illustration of the trapezoidal filter shape. Inside the interval [-T,-A] the filter has positive slope, inside the interval [-A, A] the slope has positive parameters and slope has negative inside the interval [A, T]

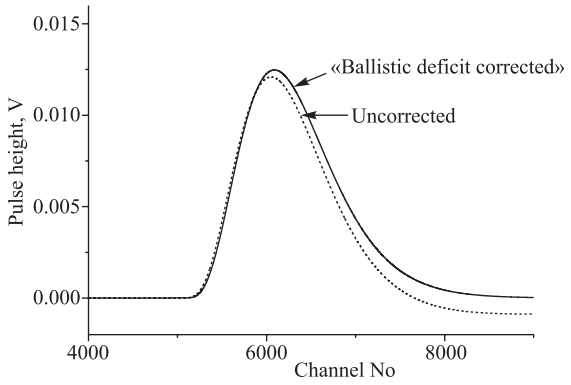

Fig. 8. Output pulse of the CR-RC^4 filter when a step-like pulse is applied to the input

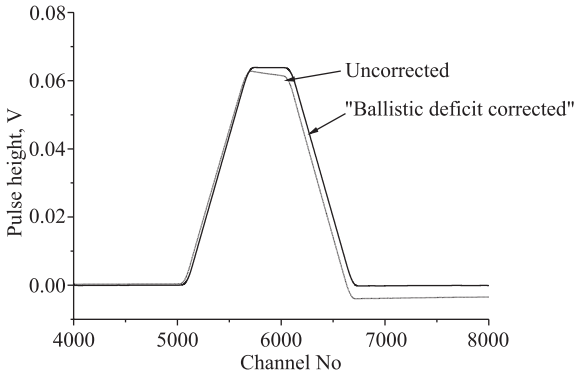

Fig. 9. Output pulse of the trapezoidal filter when a step-like pulse is applied to the input

shown in Figs. 8 and 9, respectively. As an example, a pulse height distribution for a ^{60}Co source using a HPGe as detector and the oscilloscope, presented in Fig. 10, is acquired using the CR-RC^4 shaping algorithm. The resolution was found to be 2.15 keV. It should be noted that the activity of the source was not high enough to create a considerable pile-up rate in order to investigate the influence of the source intensity on the quality of the implemented signal processing. Therefore, a special procedure was developed to verify the effectiveness of the pile-up elimination algorithm on the quality of the obtained pulse height distributions.

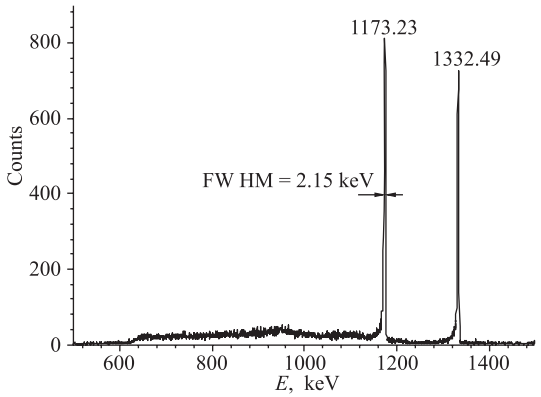

Fig. 10. Energy spectrum constructed from waveforms acquired during a measurement with a ^{60}Co calibration source

INVESTIGATION OF PILE-UP ELIMINATION SCHEME

The measurement procedure considered above works well for isolated pulses, i.e., pulses separated from each other by a distance longer than the width of the response of the CR-RC^n or trapezoidal filter to the unit step pulse. In practice, complete pulse isolation cannot be realized and as a result some pulses were distorted by pile-up. To prevent the measured spectrum degradation, a special pile-up elimination procedure was developed and implemented in measurements. First, the output signal of the charge-sensitive preamplifier was converted to a current pulse using Eq. (10). According to the used data acquisition scheme, the pulse triggering the acquisition hardware was located at a fixed position of the waveform called trigger position. If an additional pulse was detected at the distance less than $\pm$L, then the acquired waveform undergoes the pile-up elimination procedure illustrated in Fig. 11. The area occupied by the detected pile-up pulse in the waveform (right-hand part of Fig. 11) was forced to zero and then the target pulse height was calculated using pulse processing with the

CR-RC^4 or the trapezoidal shaping as was described in the previous paragraph. Unfortunately, even though forcing the area in the vicinity of the analyzed pulse to zero does not affect the pulse itself, it influences the noise, eventually degrading the resolution of the spectrometer. Obviously, the scale of such an influence can be investigated by comparing the spectrometer resolution, when pile-up flagged waveforms are completely excluded from the analysis, with the resolution, when the pile-up elimination scheme was implemented. As was mentioned above at the available source intensity, almost 100% of the acquired events were free of pile-ups. Therefore pile-up pulses were simulated by forcing of the average signal width time interval to zero and the resolution was compared with the resolution measured with undisturbed waveforms. The distance between the analyzed pulse and the simulated pile-up was fixed to a certain value and the entire acquired data set was analyzed to determine the resolution for the 1.173 MeV line of the ^{60}Co source. The procedure was repeated with different distances between the pulse and the simulated pile-up, and the dependence of the resolution on the distance was measured and plotted in Figs. 12 and 13 for the CR-RC^4 and for the trapezoidal filters, respectively.

The degradation of the spectrometer resolution as shown in Figs. 12 and 13 is stipulated by the distortion of the electronic noise, when the pile-up elimination

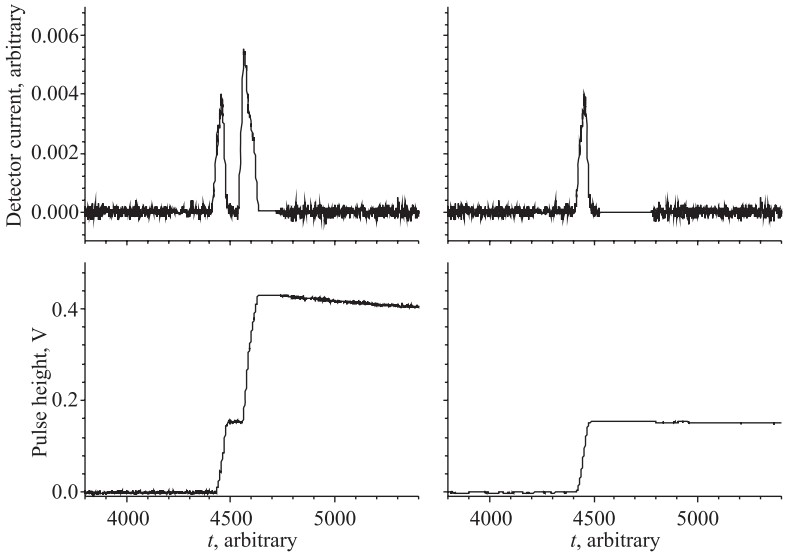

Fig. 11. The sequence of steps in pile-up elimination using a current pulse waveform starts from pile-up detection as shown in the upper left figure. Elimination of the second current pulse is demonstrated in the upper right figure. The lower two figures illustrate the conversions of the $Q(t)$ waveform

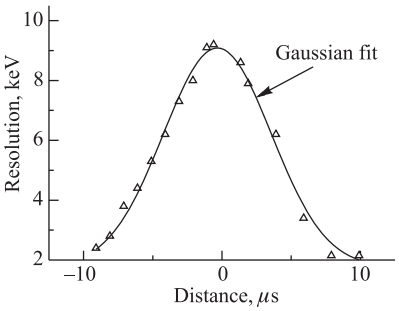

Fig. 12. Resolution as a function of the distance between the original pulse and the simulated pile-up pulse for the CR-RC^4 filter

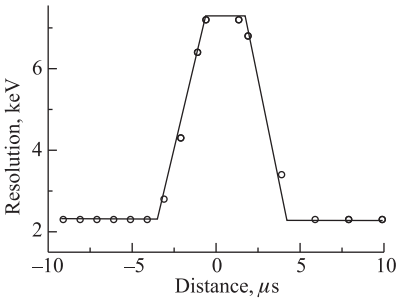

Fig. 13. Resolution as a function of the distance between the original pulse and the simulated pile-up pulse for the trapezoid filter

scheme is implemented. In real measurements pile-up pulses also cause degradation of resolution and one might raise the question about the relation between these two effects. It should be noted that the resolution degradation in the case of using the described pile-up elimination scheme depends on the distance between pulses and at the minimum distance (when pulses still can be treated as separate) it is ~ 3 times (for trapezoidal filter) lower than for isolated pulses. Such degradation, however, can be controlled by the software, and therefore the experimentalist can make a choice between the counting rate and the resolution in his measurement.

For fission fragment mass spectroscopy, the double back-to-back Frisch-gridded ionization chamber has an intrinsic energy resolution of ~ 600 keV [10]. The contribution of the electronic noise to this value measured with the help of a precision pulse generator was found to be ~ 50 keV. Taking into account the results of the HPGe detector measurements, one can expect almost no degradation of the resolution for fission fragment spectroscopy when the pile-up elimination scheme will be implemented. This conclusion can open new perspectives for fission fragment mass and kinetic energy measurements of targets with high intrinsic alpha radioactivity such as ^{239}Pu, ^{241}Am, ^{245}Cm because the pile-up elimination scheme does not significantly influence the final energy resolution of the spectrometer.

DIGITIZATION, SAMPLING NOISE AND NUMBER OF BITS

The measurement was performed using a high purity germanium (HPGe) detector and the TDS3054B oscilloscope (ENOB = 6.2) as the waveform digitizer. The energy resolution determined from the spectrum being 2.15 keV FWHM for the 1.173 MeV line of the ^{60}Co source was achieved with an RC-CR^4 shaping.

The parameter A $= 4000$ ns was chosen both for differentiator (Eq. 12) and integrator (Eq. 13). For comparison the procedure described in Ref. 11 was implemented for the analysis of the same data set, where the pulse height was calculated as the difference between values averaged in two windows of the same width selected at the fixed position and symmetrically in respect to the step. From calculation point of view, the last procedure seems similar to the trapezoidal filtering considered above. The difference is that in the analysis with a trapezoidal filter the maximum value of the difference is selected between sequential values calculated for moving windows, but the procedure of Ref. 11 gives the difference at a predefined point, which cannot guarantee the maximum for any waveform. Using widths of both windows of 10000 ns selected symmetrically in respect to the trigger position, a FWHM of 2.90 keV for the 1.173 MeV line of the ^{60}Co source was obtained, which is more than 40% worse than in the analysis with a trapezoidal filter. The first reason of degradation of the resolution is that the procedure described in Ref. 11 does not guarantee the best SNR value according to Ref. 12 (the best SNR can be achieved at the peak of the filtered signal). The second reason is that the present filtering procedure, in contrary to the procedure with fixed positions of the windows, utilizes the full dynamic range of the signal including its rising edge. Apparently, a signal dynamic range limitation reduces the ENOB of the WFD increasing the sampling noise. Comparison of different signal processing results are summarized in the Table, where the resolution is determined both for signals from the gamma source and for fixed pulse height signals from the precision pulse generator.

As can be seen, the energy resolution of a spectrometer based on HPGe detectors depends on electronic noises which can be considered as parallel and serial white noise generators at the input of the preamplifier [12]. For the considered digital spectrometer, additional sampling noises introduced by the WFD should be taken into account, too. The sampling and electronic noises are obviously uncorrelated and their effect on the detector resolution is additive. As was mentioned above the definition of ENOB according to Eq. (7) includes both sampling and apparatus generated (differential nonlinearity, missing codes, temperature drift, of the analogue-to-digital converter, etc.) fluctuations, which also can be considered as noises. Let us consider a step pulse applied to the preamplifier input using a pulse generator shown in Fig. 1. Assuming unity pulse height at the output of the preamplifier and presuming that the noises being homogeneously distributed random functions with ENOB at the input of the spectrometer, one can determine the SNR improvement after passing the digital SFA using the following equation from Ref. 13

$$S_y(f) = |W(f)|^2 S_x(f), s_y(t) = \int_0^\infty w(t-\chi) s_x(\chi) d\chi, \tag{19}$$

$S_x(f)$ and $S_y(f)$ are supposed to be power spectra of the input $s_x(t)$ and the output $s_y(t)$ signals, respectively, and $W(f)$ is the frequency response function of the spectrometer. Equation. (19) can be used both for the noise and the signal power spectrum transformation after passing the SFA with the weighting function $w(t)$.

$$w(t) = \frac{1}{2\pi}\int_0^\infty W(f)\exp(i2\pi ft)df, W(f) = \int_0^\infty w(t)\exp(-i2\pi ft)dt, \quad (20)$$

$$s_y(t) = \frac{1}{2\pi}\int_0^\infty S_y(f)\exp(i2\pi ft)df, s_x(t) = \frac{1}{2\pi}\int_0^\infty S_x(f)\exp(i2\pi ft)df. \quad (21)$$

For example, the step-like pulse $v_x(t) = 1 - \exp(-\frac{t}{\tau})$ having an exponentially rising front edge has the frequency dependent power spectrum:

$$|V_x(f)|^2 = \sqrt{\frac{2}{\pi}}\frac{\tau}{1+4\pi^2 f^2\tau^2}. \quad (22)$$

Due to the uniform noise power spectrum of the noises the SNR for the $v_x(t)$ has a frequency dependence given by Eq. (22). Such a dependence can be reduced by the appropriate choice of the weighting function $W(f)$, being the optimal weighting filter. Detector pulses have variable shape, which makes the frequency power distributions different for different pulses. That is why the realization of the matched [14] filter is practically impossible in analogue signal processing. Availability of every signal waveform, in principle, creates the conditions for a matched filter (matched filter has the target signal as the kernel of the filter) to be implemented for each individual pulse in the DSP analysis. The matched filter is optimal in the sense that the top of the peak is farther above the noise than can be achieved with any other linear filter. The practical realization of the matched filter stipulates for the FFT algorithm implementation making data analysis program very complicated and therefore impractical. It should be noted that for many applications the RC-CR^n filter is as close to the matched filter as larger the difference between signal raise and the exponential fall times gets. The quality of different filters can be compared by measuring the SNR (or the energy resolution) of the pulses stimulated by particles with a fixed energy. In practice the SNR determination can be performed using the measured value for the FWHM of the mono-energetic gammas (or using the precision pulse generator) for different weighting functions implemented in digital SFA. The output pulse height at the preamplifier output, when measuring the signal from a generator, was chosen to be approximately 150 keV higher than the 1173 keV ^{60}Co source line. Results of measurements are presented in the Table and show the same result

for a generator pulse analyzed with the CR-RC^4 and the trapezoidal filters which are smaller than the resolution of the ^{60}Co γ-ray line presented in the last row.

Energy resolution for different SFA measured using the pulse generator and a ^{60}Co source

Filter	Res. measured with high precision pulse generator [keV]	Resolution of (1173.2 keV) line [keV]
CR-RC^4	1.40	2.15 («ballistic deficit» corrected)
Trapezoidal	1.40	2.20 («ballistic deficit» corrected)
Ref. [11]	2.00	2.90 («ballistic deficit» not corrected)

Calculating the SNR for signals after passing the SFA one can raise the question how it became possible to obtain a precision of 1.4 keV using a WFD having only 6.2 ENOB. The answer is given by considering the right-hand part of Eq. (19) showing the noise transformation after passing an SFA with a weighting function $w(t)$. According to this relation, each sample of the output signal $s_y(t)$ was made of the sum of the samples of the input signal $s_x(t)$ weighted by the $w(t)$. Therefore the statistical accuracy of the output signal improved in proportion to the square root of the number of samples of the output signal involved in the calculation, which is proportional to the width of the weighting function $w(t)$. With a sampling frequency of 250 MHz and with a width of the weighting function of ~ 10 μsec used in the data analysis with a RC-CR^n – SFA ~ 2500 samples of the input function were used to calculate one sample of the output function giving an improved SNR by a factor of 50. The authors of Ref. 3 called this improvement the «bit gain factor» comparing the WFD based spectrometer with a conventional peak sensing ADC based analogue spectrometer. Following that approach, the spectrometer used in the present work had the same SNR as a 11.84 bit conventional peak sensing ADC.

CONCLUSIONS

Signal processing algorithms developed in this work were provided as recursive computational procedures that can be effectively used for computation. Comparison of developed algorithms with that described in literature showed almost 40% improvement of the resolution in high resolution gamma-spectroscopy. From the sampled waveform of a detector signal amplified by a charge-sensitive preamplifier the detector current signal was first reconstructed and was used for pile-up elimination and true ballistic deficit correction of the detector charge. The

pile-up elimination method was found to be very effective for fission fragment spectroscopy, although not demonstrated in the present paper. The basics of the signal sampling theory were briefly reviewed to demonstrate the method of calculation using sampled signal representation in the analysis procedure where the signal values are to be reconstructed between sample points.

Acknowledgements. One of us (S. Z.) would like to thank the European Commission for the support to perform this research as a Detached National Expert at the JRC-IRMM.

REFERENCES

1. *Georgiev A., Gast W.* // IEEE Trans. Nucl. Science 1993. V. 40. P. 773–779.
2. *Paula A. et al.* // Nucl. Instr. and Meth. A. 2000. V. 439. P. 378–384.
3. *Bardelli L. et al.* // Nucl. Instr. and Meth. A. 2006. V. 560. P. 517–523.
4. *Kihm T. et al.* // Nucl. Instr. and Meth. A. 2003. V. 498. P. 334–339.
5. *Kalinin A. I. et. al.* // Instr. and Meth. A. 2005. V. 538. P. 718–722.
6. TekVisa Connectivity Software V3.0.2 build 33, www.tektronix.com
7. *Max. J.* Méthodes et techniques de traitement du signal et applications aux mesures physiques. Troisième Edition, MASSON, 1981.
8. Analog Devices, Fundamentals of Sampled Data Systems, Application note AN-282.
9. *Vaseghi S. V.* Advanced Digital Signal Processing and Noise Reduction. Second edition. John Willey & Sons Ltd, 2000.
10. *Budz-Jørgenson C. et al.* // Nucl. Instr. and Meth. A. 1987. V. 258. P. 209.
11. *Khriachkov V. A. et al.* // Nucl. Instr. and Meth. A. 2000. V. 444. P. 614–621.
12. *Radeka V.* // IEEE Trans. Nucl. Science 1968. V. 15. P. 455–470.
13. *Bendat J. S., Piersol A. G.* Measurement and Analysis of Random Data. John Wiley & Sons, Inc., 1966, P. 99.
14. *Smith S. W.* The Scientist and Engineer's Guide to Digital Signal Processing, available at http://www.dspguide.com/.

Received on December 21, 2007.

Редактор *Э. В. Ивашкевич*

Подписано в печать 05.03.2008.
Формат 60 × 90/16. Бумага офсетная. Печать офсетная.
Усл. печ. л. 1,25. Уч.-изд. л. 1,78. Тираж 290 экз. Заказ № 56102.

Издательский отдел Объединенного института ядерных исследований
141980, г. Дубна, Московская обл., ул. Жолио-Кюри, 6.
E-mail: publish@jinr.ru
www.jinr.ru/publish/